http://dx.doi.org/10.5012/bkcs.2012.33.9.2855

Articles

Electrostatic Properties of *N*-Acetyl-Cysteine-Coated Gold Surfaces Interacting with ZrO_2 Surfaces

Jin-Won Park

Department of Chemical & Biomolecular Engineering, School of Energy and Biotechnology, Seoul National University of Science and Technology, Seoul 139-743, Korea. E-mail: jwpark@seoultech.ac.kr
Received February 15, 2012, Accepted April 4, 2012

The coating *N*-acetyl cysteine (NAC) on gold surfaces may be used to design the distribution of either gold particle adsorbed to the ZrO_2 surface or *vice versa* by adjusting the electrostatic interactions. In this study, it was performed to find out electrostatic properties of the NAC-coated-gold surface and the ZrO_2 surface. The surface forces between the surfaces were measured as a function of the salt concentration and pH value using the AFM. By applying the Derjaguin-Landau-Verwey-Overbeek (DLVO) theory to the surface forces, the surface potential and charge density of the surfaces were quantitatively acquired for each salt concentration and each pH value. The dependence of the potential and charge density on the concentration was explained with the law of mass action, and the pH dependence was with the ionizable groups on the surface.

Key Words : *N*-Acetyl cysteine, Gold surface, ZrO_2 surface, AFM, DLVO theory

Introduction

Materials composed of gold and a semiconducting support such as ZrO_2 are considered for numerous applications for example in surface patterning,[1] hydrogenation,[2,3] and CO oxidation.[4] In the latter case, the excitation of the semiconductor-metal nanocomposite by CO adsorption that may be utilized for the activation of oxygen,[5] *i.e.* for the production of carbon dioxide by oxygen splitting. Activity and selectivity of such materials and catalysts rely on the distribution.[6]

Different approaches were used in the past to prepare gold/oxide catalyst materials such as metal ion impregnation and deposition-precipitation followed by drying, calcinations, and reduction.[7-9] These procedures lead to the formation of gold particles or clusters on the support. However, these approaches have some disadvantages. The uneven precursor-solution loading due to gravitational forces results in variation in the size of metal particles. The thermal treatment causes severe agglomeration problems and may even cause chemical modification of the support through ionic diffusion.[6] Therefore, alternative routes for catalyst preparation are suggested.[10] A different approach relates to the preparation of metallic gold particles in solution and subsequent deposition on the oxide. This approach is based on passivating ligands such as phosphines and thiols, which prevent the particles from agglomeration in solution.[11,12] Gold particles are deposited on the oxide, followed by the calcinations to remove the passivating ligands.[13-15]

The atomic force microscope has opened up new era for the direct measurement of the interaction between a colloidal particle and a flat surface as a function of separation.[16] By fitting these force-separation curves with Derjaguin-Landau-Verwey-Overbeek (DLVO) theory,[17] it is possible to obtain the electrostatic properties of the surface being studied. These surface properties are an indicator to represent electrostatic repulsive force between particles, which may strongly affect on the particle distribution that is critical to the activity and selectivity of the catalyst. In this research, we aim to find out electrostatic properties of the *N*-acetyl cysteine (NAC)-coated-gold surfaces and the ZrO_2 surfaces with respect to the salt concentration only.

Experimental

Surface Preparation. The gold surfaces were prepared by using a high-vacuum electron beam evaporator to sequentially deposit a 5 nm chrome adhesion layer and a 100 nm gold layer on the silicon wafers. Immediately prior to use, the gold surfaces were cleaned in a 4:1 solution of 96% sulfuric acid and 30% hydrogen peroxide at 60-80 ^{o}C for 5 min. The coating of NAC layer was coated by the immersion of the gold surface in a solution of 10 mM NAC, 100 mM potassium nitride, at pH 4 for several hours at room temperature, followed by rinsing with a running buffer. In order to prove that only the adjustment of the salt concentration is able to control the interaction between the NAC-coated surface and the other metal surface, all of the NAC immobilization was conducted at 100 mM potassium nitride. Therefore, the Hamaker constant of the surface was not varied. The immobilization of NAC was confirmed from qualitative surface force measurement in 100 mM potassium

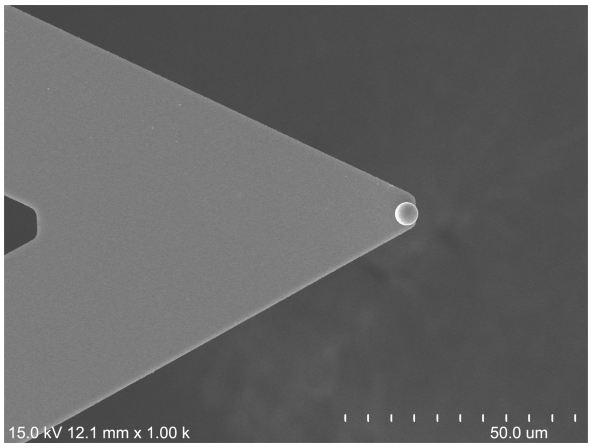

Figure 1. Zirconia sphere-attached-cantilever.

nitride at pH 4.

For quantitative surface force measurements, the solution was replaced with a running buffer (There are six running buffers used in this research - 100, 10, and 1 mM potassium nitride at pH 4 and 8, respectively). Deposition of zirconia layer was performed on the surface of the silicon wafer by sputtering zirconium in an argon-oxygen environment for 41 min using an RF Magnetron source operating at 2 kW. Prior to sputtering, the wafer surfaces were cleaned with hydrofluoric acid to remove any native oxide layer. The total pressure used was 5×10^{-6} bar, with argon and oxygen flow rates of 6 and 1.2 dm^3/min, respectively. The substrate was rotated continuously during sputtering and distant to the 20 diameter target by 7 cm. The characteristics of the zirconia layers were identical with those of the gold surface.

AFM Measurements. Topology images and surface force measurements were made with a 3-D Molecular Force Probe AFM (Asylum Research, Santa Barbara, CA) with a closed-loop piezo-electric transducer. Microfabricated silicon oxynitride cantilever (Olympus, Shinjuku-ku, Tokyo, Japan) with 20 nm radius tip were used for topographic imaging and qualitative surface force measurements. Surface force measurements were quantitatively made with zirconia spheres (Microspheres-Nanospheres, Cold Spring, NY) of 3 μm diameter that were attached to the microfabricated cantilevers, shown in Figure 1. The spheres were immobilized at the end of the cantilever with UV-sensitive adhesive (Norland Products, New Brunswick, NJ). Exposure to the UV light source and surface cleaning were achieved in an ozone cleaning apparatus (Jelight, Irvine, CA). It was confirmed that the UV exposure did not cause any change in the response of the cantilever. The spring constant of the cantilever was acquired from the thermal frequency spectrum of the cantilever.[18]

Theory

Theories for the forces between interacting electrostatic double layers have been described by numerous authors. The interaction between similarly charged double layers at low surface potentials is explained by the theory of Derjaguin-Landau-Verwey-Overbeek (DLVO).[19] According to DLVO theory, the total interaction energy between two plates can be considered as the sum of several contributions, including an attractive van der Waals component (V_A) and an electrostatic repulsion or attraction (V_E). Considerable evidence has been suggested for an additional repulsion (V_S) at close separations resulting from the presence of ordered solvent layers.[20-23]

Using the Derjaguin approximation,[24] the force between spheres of radius R_T can be related to the energy between plates by the expression

$$F/R_T = 2\pi(V_A + V_E + V_S) \tag{1}$$

The van der Waals energy (V_A) in the non-retarded limit is described by an equation of the form

$$V_A = -A_H/12\pi d^2 \tag{2}$$

where A_H is the Hamaker constant and d is the separation distance.[25] The Hamaker constant of the NAC layer is assumed to be 7.0×10^{-20} J, because the layer is made with hydrocarbon.[26] The Hamaker constant of the zirconia surface is 10.0×10^{-20} J.[27] The electrostatic interaction (V_E) can be derived by considering the free energy associated with the formation of a double layer or by integrating the electrostatic force.[28-30] Using the latter method, the interaction for a 1:1 Electrolyte is

$$V_E = -\int_{\infty}^{D} \left\{ 2n^0 kT\left[\cosh\left(\frac{ze\psi}{kT}\right)-1\right] - \frac{\varepsilon}{2}\left(\frac{d\psi}{dz}\right)^2 \right\} dz \tag{3}$$

where ψ is the electrostatic potential. In Eq. (3), the first term represents a repulsive osmotic component that results from the charge accumulation between the plates, and the second is a Maxwellian stress that represents an induced charge and is always attractive. For similarly charged surfaces, the second term disappears, leaving a results equivalent to DLVO. To determine V_E explicitly, the electrostatic potential must be known. This can be found by solving the Poisson-Boltzmann equation

$$\frac{d^2\psi}{dz^2} = -\frac{1}{\varepsilon_0\varepsilon_r}\sum_i n_i^0 z_i e \exp\left(-\frac{z_i e\psi}{kT}\right) \tag{4}$$

Generally, the solution of Eq. (4) must be acquired only by numerical techniques, and the calculation of Eq. (3) was then conducted with a Simpsons' 3/8 rule.[31] The additional repulsive force (V_S) in Eq. (1) is thought to arise from the presence of ordered solvent layers and can be described by a decaying oscillatory force.[32] However, this repulsive force is not clearly understood and will be neglected in the calculations presented here.

Results and Discussion

The constant force mode of the AFM was used to characterize the structures of the NAC layer formed on the gold surfaces. AFM images were acquired on the gold surfaces,

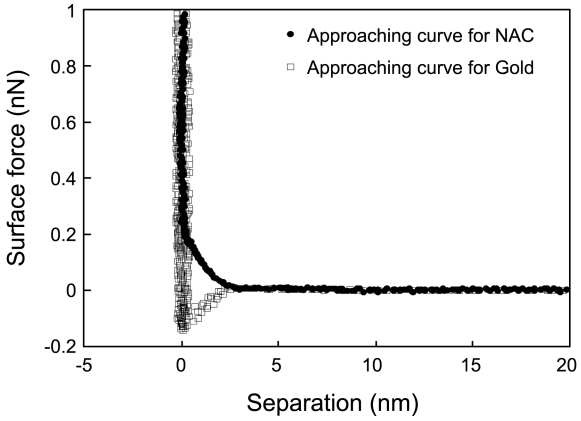

Figure 2. Force-distance curve between a silicon nitride probe and the N-acetyl-cysteine (NAC) layer formed in 100 mM potassium nitride at pH 4.

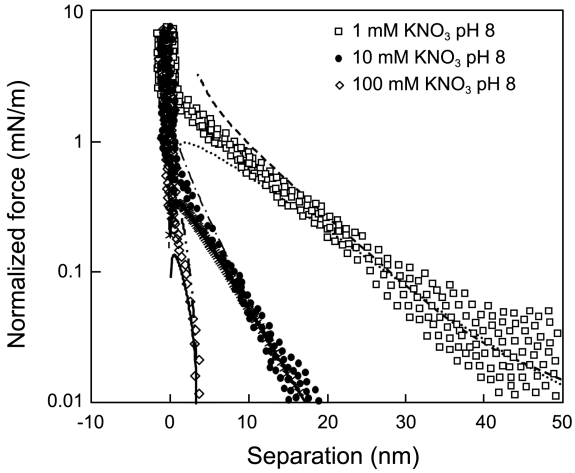

Figure 3. Approaching force curve as a function of the separation between the sphere and the surface of the zirconia in 1, 10, 100 mM potassium nitride at pH 8.

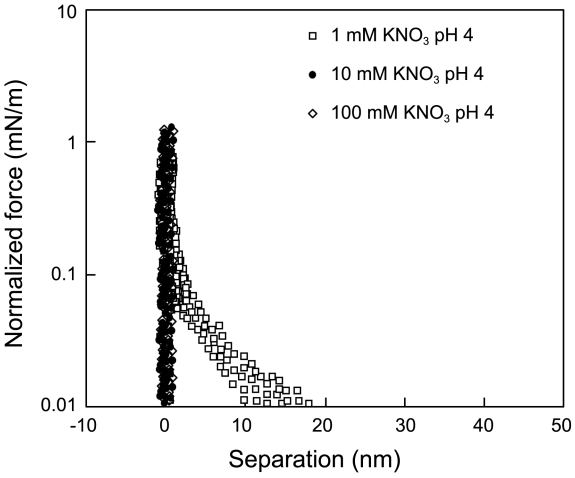

Figure 4. Approaching force curve as a function of the separation between the sphere and the surface of the zirconia in 1, 10, 100 mM potassium nitride at pH 4.

NAC-coated gold surfaces, and zirconia surfaces. The morphologies of the gold surfaces, the NAC-coated gold surface, and the zirconia surfaces were dominated by the polycrystalline structure of the evaporated metals and indistinguishably rough about 1.5 nm (results were not shown). Phase separation in lipid and fatty acid films has been observed with AFM and is easily visualized as micrometer-sized domains in the contact imaging mode.[33] The fact that domains were not observed on the NAC-coated gold surfaces is strong evidence that the NAC forms homogeneous layer on the gold surfaces.

Since the morphology was indistinguishable between the NAC layer and the gold surface, AFM force measurements on the surfaces were used with 20-nm-radius probes in order to confirm the formation of NAC layer on the gold surfaces. Figure 2 presents approaching force-distance measurements between a silicon nitride probe and the NAC layer formed in 100 mM potassium nitride at pH 4. The observed forces were purely short-range-repulsion below around 2.0 nm at loads of approximately 0.2 nN, while the force curve of the gold surface showed an attractive region. The repulsion, not found on the gold surfaces, appears in the NAC layer, because the NAC layer has the lower Hamaker constant and the more hydration.[26] The clear difference of the force curve indicates that the NAC layers were well-formed on the gold surfaces.

For the quantitative characterization of the NAC-coated-gold surface properties, the surface charge density and potential of the 3-μm-diameter zirconia sphere were found as a first with the force measurements between the sphere and the zirconia surface. Figure 3 presents the approaching surface force curves as a function of the separation between the zirconia sphere and the zirconia surface in three running buffers at pH 8. The long-range surface forces were purely repulsive, and their range was highly dependent on the ionic strength of the solution. The exponential dependence of the repulsive force on distance was consistent with double-layer forces between surfaces of like charge in aqueous solutions. At separations of less than 2 nm, significant short-range repulsive forces were observed and believed to arise from the steric forces and the inherent roughness of the surfaces.[34,35] However, the behavior of surface forces at pH 4 was different from that at pH 8 (Figure 4). The repulsive forces, observed in 1 mM potassium nitrate solution at pH 4, were smaller than those at pH 8 due to the iso-electric point of zirconia. The forces, found at pH 8, were not observed in 10 mM and 100 mM potassium nitrate solution at pH 4. That is, in 10 mM and 100 mM potassium nitrate solution at pH 4, the electrostatic forces in the long range appeared not to be the dominant component of the surface forces on the zirconia surface. Therefore, in 10 mM and 100 mM potassium nitrate solution at pH 4, it was not appropriate to apply the DLVO theory to the force curves so that the surface potential and charge density could be acquired.

The analysis with the DLVO theory was conducted for the long-range surface forces using either constant surface potential or charge density boundary conditions. The results of these calculations are summarized in Table 1. The surface potential of the zirconia surface is on the order of −10 to

Table 1. Electrostatic properties of the zirconia surfaces

	pH 8		
	1 mM Potassium nitrate	10 mM Potassium nitrate	100 mM Potassium nitrate
Surface potential (mV)	−37 ± 4	−24 ± 3	−16 ± 2
Surface charge density (10^{-3} C/m^2)	−2.5 ± 0.3	−6.0 ± 0.6	−10.5 ± 1.3
	pH 4		
	1 mM Potassium nitrate	10 mM Potassium nitrate	100 mM Potassium nitrate
Surface potential (mV)	+8 ± 1	–[a]	–[a]
Surface charge density (10^{-3} C/m^2)	+0.6 ± 0.2	–[a]	–[a]

[a]Electrostatic property was not acquired.

−100 mV at pH 8.0. The result appears to be consistent with that of Choi *et al*.,[36] where electrophoretic technique was used to characterize the charge state of the zirconia surface. The change from negative potential to positive potential is due to change from negative to positive values at an isoelectric point of pH 5.5.[37] For the 10 mM and 100 mM potassium nitrate solution at pH 4, the surface potential and charge density of the zirconia surface were not acquired.

As summarized Table 1, it can be seen that the ionic strength at pH 8 decreased monotonically with the potential increase and the charge density decrease of the zirconia surface. Pashley has developed a model to explain the salt concentration dependence of the surface potential and charge density of a surface with ionizable groups based on the law of mass action.[38] The interrelation between charge density (σ), surface potential (ψ_o), and salt concentration may be determined by the simultaneous solution of the law of mass action

$$\sigma = \sigma_o \frac{1}{1 + K_a[H^+]\exp\left(-\frac{e\psi_o}{kT}\right) + K_{K^+}[K^+]\exp\left(-\frac{e\psi_o}{kT}\right)} \quad (5)$$

and Graham's equation

$$\sigma = \sqrt{8\varepsilon\varepsilon_o kT}\,\sinh\left(\frac{e\psi_o}{kT}\right)\sqrt{([K^+]+[H^+])} \quad (6)$$

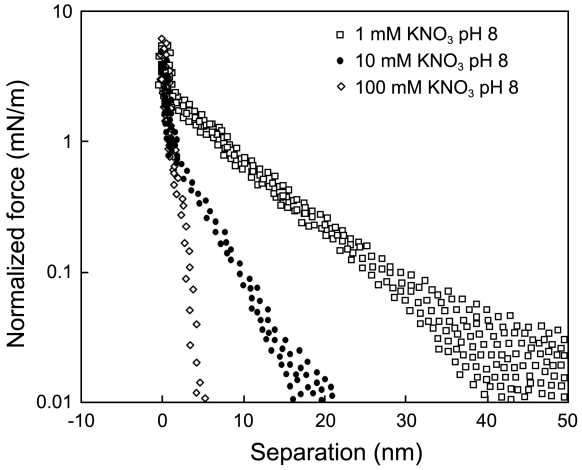

Figure 5. Approaching force curve as a function of the separation between the zirconia sphere and the NAC layer in 1, 10, 100 mM potassium nitride at pH 8.

where σ_o is the maximum surface charge density, ψ_o is the surface potential, ε is the dielectric constant of water, ε_o is the permittivity of free space, e is the electronic charge constant, k is the Boltzmann's constant, T is temperature. The surface potential and charge density relation to the salt concentration found at pH 8.0 were identical to the trends predicted by Pashley's model. For the purpose of this study, the zirconia surface potential and charge density from the

Table 2. Electrostatic properties of the *N*-acetyl-cysteine (NAC) layer

	pH 8		
	1 mM Potassium nitrate	10 mM Potassium nitrate	100 mM Potassium nitrate
Surface potential (mV)	−80 ± 7	−51 ± 5	−32 ± 3
Surface charge density (10^{-3} C/m^2)	−13 ± 2	−25 ± 3	−46 ± 5
	pH 4		
	1 mM Potassium nitrate	10 mM Potassium nitrate	100 mM Potassium nitrate
Surface potential (mV)	−20 ± 2	–[a]	–[a]
Surface charge density (10^{-3} C/m^2)	−1.5 ± 0.2	–[a]	–[a]

[a]Electrostatic property was not acquired.

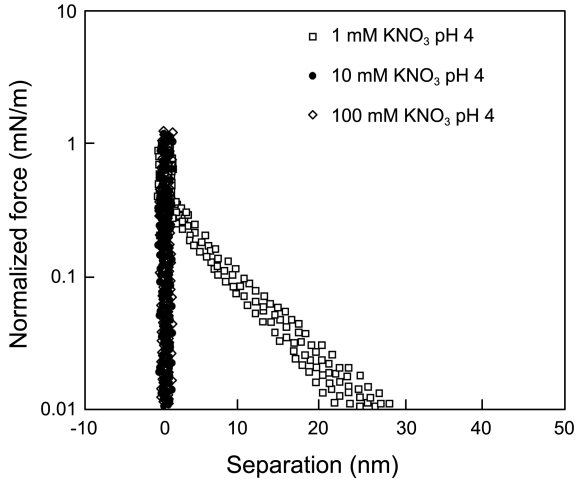

Figure 6. Approaching force curve as a function of the separation between the zirconia sphere and the NAC layer in 1, 10, 100 mM potassium nitride at pH 4.

DLVO theory analysis to the experiment data were used to characterize the NAC layer formed on the gold surfaces.

The surface potential and charge density of the NAC layer formed on the gold surfaces were characterized by making surface force measurements on them with the zirconia sphere. Figure 5 shows the surface forces between the NAC layers and the zirconia sphere in the three running buffers at pH 8. The long-range surface forces were purely repulsive and varied in range with ionic strength in a manner that was consistent with double-layer forces. Quantitative analysis of the surface forces with the DLVO theory was performed using asymmetric boundary conditions. As summarized in Table 2, the surface potential and charge density of the NAC layer also depend on the salt concentration consistently with Pashley's model. It was observed that the surface charge densities and potentials of the NAC layer were much larger than those for the zirconia surfaces at pH 8, which can be attributed to the ionized-functional-groups of the NAC layer. The long range forces were purely attractive in 1 mM potassium nitrate solution at pH 4, as shown in Figure 6. This attraction was expected, considering pK_a of the NAC and the iso-electric point of zirconia. The long range forces were not observed in 10 mM and 100 mM potassium nitrate salt concentrations at pH 4, which was consistent with the fact that there were no long range forces on the zirconia surfaces.

The observations described above suggest that the electrostatic forces between the NAC-coated gold surfaces and zirconia surfaces were found to be adjustable quantitatively with a salt concentration and pH value. This adjustment means the other adjustment for the kinetics of the adsorption (either zirconia particles to NAC-coated-gold surface or NAC-coated-gold particles to zirconia surface), because the adsorption is determined by the surface forces between the surfaces. Additionally, the kinetics determines the distribution of the particles adsorbed to the surface. Therefore, the surface forces as a function of the salt concentration and the pH value seem to be important for the design of the distribution of the particles adsorbed to the surfaces, which can affect on the efficiency of catalysts.

In conclusion, the interactions between the NAC-coated-gold surface and the zirconia surface were investigated as a function of the salt concentration and pH value using the AFM. By applying the DLVO theory to the surface forces, the surface potential and charge density of the surfaces were quantitatively acquired for each salt concentration and each pH value. The surface potential and charge density dependence on the salt concentration was explained with the law of mass action, and the pH dependence was with the ionizable groups on the surface. And the coating *N*-acetyl cysteine on gold surfaces may be used to design the distribution of either gold particle adsorbed to the zirconia surface or vice versa by adjusting the electrostatic interactions.

Acknowledgments. This study was financially supported by Seoul National University of Science and Technology. We thank all of members of Department of Chemical & Biomolecular Engineering, the Seoul National University of Science and Technology for help and valuable discussions.

References

1. Soolaman, D. M.; Yu, H.-Z. *J. Phys. Chem. C* **2007**, *111*, 14157.
2. Hugon, A.; Delannoy, L.; Louis, C. *Gold Bull.* **2008**, *41*, 127.
3. Zhang, X.; Shi, H.; Xu, B.-Q. *J. Catal*. **2011**, *279*, 75.
4. Wang, C.-M.; Fan, K.-N.; Liu, Z.-P. *J. Am. Chem. Soc.* **2007**, *129*, 2642.
5. Arrii, S.; Morfin, F.; Renouprez, A. J.; Rousset, J. L. *J. Am. Chem. Soc*. **2004**, *126*, 1199.
6. Zhang, X.; Wang, H.; Xu, B. Q. *J. Phys. Chem. B* **2005**, *109*, 9678.
7. Kamat, P. V. *J. Phys. Chem. C* **2007**, *111*, 2834.
8. Valden, M.; Lai, X.; Goodman, D. W. *Science* **1998**, *281*, 1647.
9. Sakurai, H.; Tsubota, S.; Haruta, M. *Applied Catalysis A-General* **1995**, *102*, 125.
10. Li, X.; Fu, J.; Steinhart, M.; Kim, D. H.; Knoll, W. *Bull. Korean Chem. Soc.* **2007**, *28*, 1015.
11. Schmid, G. *Chem. Rev.* **1992**, *92*, 1709.
12. Noh, J.; Park, H.; Jeong, Y.; Kwon, S. *Bull. Korean Chem. Soc.* **2006**, *27*, 403.
13. Dasog, M.; Scott, R. W. J. *Langmuir* **2007**, *12*, 3381.
14. Sandhyarani, N.; Pradeep, T. *Chem. Phys. Lett.* **2001**, *338*, 33.
15. Brewer, N. J.; Rawsterne, R. E.; Kothari, S.; Leggett, G. J. *J. Am. Chem. Soc.* **2001**, *123*, 4089.
16. Binnig, G.; Quate, C.; Gerber, G. *Phys. Rev. Lett.* **1986**, *56*, 930.
17. Derjaguin, B. V.; Landau, L. *Acta Physiochem.* **1941**, *14*, 633.
18. Cleveland, J. P.; Manne, S.; Bocek, D.; Hansma, P. K. *Rev. Sci. Instrum.* **1993**, *64*, 403.
19. Derjaguin, B. V. *Trans. Faraday Soc.* **1940**, *36*, 203.
20. Israelachvili, J. N.; Adams, G. E. *J. Chem. Soc. Faraday Trans.* **1978**, *74*, 975.
21. Shuin, V.; Kekicheff, P. *J. Colloid Interface Sci.* **1993**, *155*, 108.
22. Parker, J. L.; Christenson, H. K. *J. Chem. Phys.* **1988**, *88*, 8013.
23. O'Shea, S. J.; Welland, M. E.; Pethica, J. B. *Chem. Phys. Lett.* **1994**, *223*, 336.
24. Derjaguin, B. V. *Kolloid Z* **1934**, *69*, 155.
25. Hartmann, U. *Phys. Rev. B* **1991**, *43*, 2404.
26. Israelachivili, J. N. *Intermolecular & Surface Forces*; Academic Press: New York, 1991; pp 183-188, 275-282.
27. Shin, H.; Agarwal, M.; de Guire, M. R.; Heuer, A. H. *Acta Mater.* **1998**, *46*, 801-815.

28. Verwey, E. J. W.; Overbeek, J. T. G. *Theory of the Stability of Lyophobic Colloids*; Elsevier: New York, 1948; pp 51-63.
29. Hogg, R.; Healy, T. W.; Fuerstenau, D. W. *Trans. Faraday Soc.* **1966**, *62*, 1638.
30. Hunter, R. J. *Foundations of Colloid Science*; Oxford University Press: Oxford, U.K., 1987; pp 397-409.
31. Chan, D. Y. C.; Pashley, R. M.; White, L. R. *J. Colloild Interface Sci.* **1980**, *77*, 283.
32. Parker, J. L. *Surf. Sci.* **1994**, *3*, 205.
33. Park, J.-W.; Ahn, D. J. *Colloids & Surf. B: Biointerf.* **2008**, *62*, 157.
34. Ducker, W. A; Senden, T. J.; Pashley, R. M. *Nature* **1991**, *353*, 239.
35. Horn, R. G.; Smith, D. T.; Haller, W. *Chem. Phys. Lett.* **1989**, *162*, 404.
36. Choi, J. Y.; Kim, D. K. *J. Sol-Gel Sci. and Tech.* **1999**, *15*, 231-241.
37. Schultz, M.; Grimm, St.; Burckhardt, W. *Solid States Ionics* **1993**, *63-65*, 18.
38. Pashley, R. M. *J. Colloid Interface Sci.* **1981**, *83*, 531.